

ARTICLE

Microfluidic platform for directed self-assembly of droplet networks communicated via reaction-diffusion†

Cite this: DOI: 10.1039/x0xx00000x

Jan Guzowski,^{a,b} Konrad Gizynski,^a Jerzy Gorecki,^a and Piotr Garstecki^{a,*}

Received 00th January 2014,

Accepted 00th January 2014

DOI: 10.1039/x0xx00000x

www.rsc.org/

We report a microfluidic system for individually tailored generation and for incubation of core-shell liquid structures with multiple cores that chemically communicate with each other via lipid membranes. We encapsulate an oscillating reaction-diffusion Belousov-Zhabotinsky (BZ) medium inside the aqueous droplets and study propagation of chemical wave-fronts through the membranes. We further encapsulate the sets of interconnected BZ-droplets inside oil-lipid shells in order to i) chemically isolate the structures and ii) confine them via tunable capillary forces which leads to self-assembly of predefined topologies. We observe that doublets (pairs) of droplets encapsulated in the shell exhibit oscillation patterns that evolve in time. We collect statistical data from tens of doublets all created under precisely controlled, almost identical conditions from which we conclude that the different types of transitions between the patterns depend on the relative volumes of the droplets within a chemically coupled pair. With this we show that the volume of the compartment is an important control parameter in designing chemical networks, the feature previously appreciated only by theory. Our system not only allows for new insights into dynamics of geometrically complex and interacting chemical systems but is also suitable of generating autonomous chemically interconnected microstructures with possible future use, e.g., as smart biosensors or drug-release capsules.

Introduction

Here we demonstrate a microfluidic system for systematic investigation of chemical communication and information processing in droplet networks. The automated platform enables generation of individually designed sets of liquid compartments with the control over their volume, composition and geometric arrangement. The system provides a practical tool for research on chemical signalling through surfactant and lipid bilayers.

Chemical communication through membranes is one of the most important research areas in fundamental biology,¹ drug design,² chemistry³ and recently also in biochemical applications of droplet microfluidic systems.⁴⁻⁶ Experiments on chemical transport through membranes are difficult. Exploration of the largely still unknown phenomena of spatio-temporal coupling and complexity in spatially heterogeneous chemical systems requires preparation of complex architectures of liquid compartments. Ideally, both the volumes and chemical composition of these compartments should be individually adjustable, together with their relative location in space. This task, especially at the microscale and preferably at high throughput, is difficult to be performed manually.

Here we report a platform for automated generation of multiple droplets, i.e., core-shell topologies^{7, 8} with varied number and sizes of the cores⁹ containing substrates for reaction-diffusion processes. The setup facilitates rapid screening of i) the number and sizes of the liquid compartments that communicate via membranes, ii) the composition of both the cores and the membranes and iii) various arrangements of the segments, i.e., topologies of the networks. Due to reproducibility of generation of droplets in micro-channels the system that we describe allows for acquisition of statistically relevant observations from multiple parallel micro-experiments (treating each core-shell structure as a separate experiment) carried on in almost identical conditions.

We use a microfluidic device to generate and incubate arrays of multiple droplets (cores) and track the dynamics of propagation of chemical signals between them. For two cores in the shell, we classify the types of observed evolution, depending on the size ratio of the cores. We observe that the size influences the activity of the droplets which in turn leads to generation of intriguing dynamic patterns. Our results constitute a step towards microfluidic assembly and screening of interconnected droplet networks that could serve as prototype bio-compatible computing units.¹⁰

Belousov-Zhabotinsky reaction is a nonlinear phenomenon, commonly used in studies on information processing in chemical media.¹¹⁻¹³ For properly selected reagents, the concentrations of intermediate products oscillate in time. These oscillations are accompanied by periodic switching between the oxidized and the reduced form of the catalyst¹⁴ (see Fig. 1b). Since both forms have different color these changes can be easily traced optically.

Several methods for compartmentalization of the BZ-medium have been proposed. Adamatzky et al.¹⁵ used a silica gel with immobilized catalyst of a photosensitive version of the BZ medium. Illumination through a mask created a planar pattern of reaction compartments. Szymanski et al.^{16, 17} considered BZ droplets manually located in an organic oil. Thutupalli^{18, 19} encapsulated BZ medium inside emulsion droplets generated at a microfluidic junction and observed them in a two-dimensional setup. The authors observed coupling between excitations of individual droplets after chemical communication between them was established. Still, this system allowed only to generate random droplet aggregates or simple hexagonal lattices without possibility to control the topology and the geometry of the structures.

Recent work by Epstein and co-workers focused on classification of dynamic patterns in 1D^{20, 21} and 2D²² lattices of droplets assembled by microfluidics. By illuminating chosen droplets in 2D hexagonal lattices the authors were also able to isolate rings of 6 or 5 coupled droplets (exploiting a defect in the lattice in the latter case). In all of the above cases, by proper choosing the length scales (droplet diameter and spacing between droplets) and the concentration of the reagents, the authors observed either coupled phase-shifted oscillations or the morphogenetic Turing patterns. In all those demonstrations only networks of droplets of equal volumes were considered.

Here, we extend the control over volumes to the level of individual compartments. We employ the technique of on-demand generation of tiny volumes of liquids based on valves^{23, 24} which offers several new perspectives in studying dynamic chemical coupling in a compartmentalized reaction-diffusion system: i) the control parameter (droplet volume) can be changed from droplet to droplet at the time of their the generation, a feature that was not achievable in previous demonstrations, ii) topology of the network can be controlled by changing the order of generation of different volumes and by tuning the strength of capillary forces confining the droplets (the latter depending on the volume of the shell phase⁹). Assembling specific topologies of droplet networks requires setting up at least two, but preferably a higher number of arbitrarily sized and arbitrarily composed liquid compartments separated by surfactant or lipid membranes of varied properties. All of these should be done in small compartments and possibly at a fast rate. Multiple microfluidic systems for screening of membranes and membrane proteins have been already proposed²⁵ including arrays of micro-wells²⁶ separated from the bulk solution via membranes, or arrays of geometric traps holding pairs of droplets,²⁷⁻²⁹ as well systems based on automated generation and handling of droplets^{29, 30}. Here,

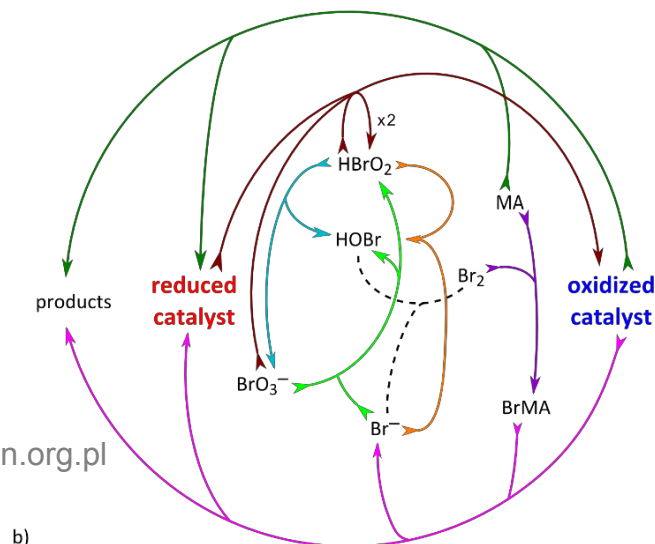
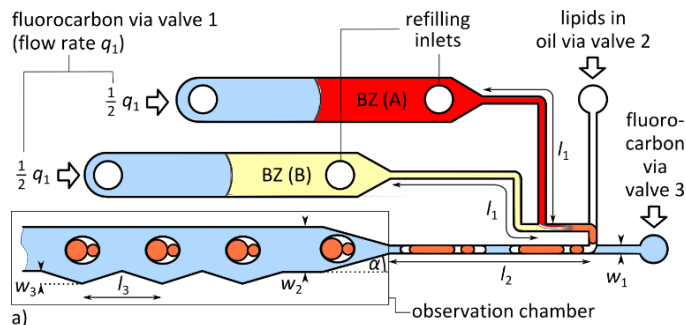


Fig. 1: a) Layout of channels on the microfluidic chip (not to scale; for technical drawing see SI). The fluorocarbon phase supplied via valve 1 pushes BZ components A and B. The 'refilling inlets' were closed during the operation of the valves. The opening angle of the inlet to the observation chamber was $\alpha \approx 30^\circ$. This smooth widening prevented fragmentation of the larger drops. The notches at the side wall of the chamber served as traps for the capsules allowing for their immobilization during monitoring of the progress of reactions. The lengths of the channels were $l_1 = 17$ mm and $l_2 = 9.5$ mm. The widths of the inlet and outlet channels at all three T-junctions were equal to $w_1 = 0.3$ mm and the depths $h_1 = 0.3$ mm. The width of the chamber was $w_2 = 2$ mm, the depth $h_2 = 2$ mm, and the sizes of the notches were $w_3 = 0.3$ mm by $l_3 = 2$ mm. b) Scheme illustrating the most important processes constituting BZ-reaction. The arrows associated with each process are marked in a different color. The black, broken line illustrates reversible formation of bromine molecule and its dissociation. MA and BrMA denote malonic acid and bromomalonic acid respectively. Red and blue fonts correspond to the actual colors of the solution periodically changing in time due to increasing concentration of either the reduced or the oxidized catalyst, respectively. In our experiments the blue color of the solution appears as nearly white (see Fig. 3) due to the small size of the drops.

instead of a geometric trap we use a drop of an immiscible oil phase to encapsulate the network of aqueous droplets. This approach allows for i) tuning the strength of confinement by changing the volume of the oil shell (which in turn impacts the topology of the network⁹) and ii) generating of multiple networks physically close to each other but being chemically isolated (by the encapsulating shells), which allows for collecting statistically relevant data. Recently, Rossi et al.³¹ reported encapsulation of BZ-droplets inside larger double emulsion drops. Tomasi et al.³² generated core-shell structures suspended in an aqueous phase each with a single BZ-core

followed by evaporation of the organic solvent from the shell resulting in formation of BZ-liposomes. These interesting techniques do not yet allow for the control over relative volumes of the cores and of the shell and for studying their impact on topology of the structures or on the resulting dynamic patterns of the reaction diffusion systems.

We employed several technical solutions to aid an efficient encapsulation, stabilization, incubation and monitoring of the progress of reactions in droplets. Some of these solutions are focused specifically on handling of the reaction-diffusion medium. As a basic illustration of the method we investigate ensembles of singlets and doublets of BZ-droplets. First, we observe that the frequency of oscillations of isolated droplets increases with their radius. Next, we use this observation to interpret the complex dependence of frequency of chemical oscillations in communicating doublets. Specifically, we analyze the relationship between the volume ratio of the droplets forming a chemically coupled pair of reactors and the firing number of forced oscillations.

Materials and Methods.

We used a microfluidic chip fabricated in polycarbonate (Macrolon, Bayer) to generate droplets and their assemblies. We milled the channels in a 5-mm thick slab via direct milling (ErgWind 4025, Poland), cleaned the piece with pressurized water (Karcher K 2.100) and rinsed it with isopropyl alcohol. We then bonded it with a second, cleaned slab, by compressing the pieces together at 130 °C for 30 min. We applied a perfluorinated oleophobic coating to the inner walls of the channels by flushing them with 3M Novec 1720, letting the solution evaporate and then baking in an oven at 100 °C for 1h.

The chip comprised a triple T-junction (Fig. 1). In the first T-junction we joined the streams of two substrates for the BZ reaction (channels l_1 in Fig. 1; we used equal lengths of the channels supplying different components in order to ensure equal hydrodynamic resistances and, consequently, equal flow rates) and immediately fed them into the second T-junction to form aqueous droplets in the shell phase (solution of lipids in an organic solvent). In the third junction the shell phase broke off to form a capsule with multiple cores.³³ We used a narrow outlet channel (l_2 in Fig. 1), such that the cores were squeezed by the walls of the channel into plugs. At this stage volumes of the droplets were proportional to their lengths (this facilitated measurement of volumes from image analysis). The plug of the shell phase containing the linear sequence of plugs-cores was flushed downstream towards a wide observation chamber in which it relaxed to the equilibrium morphology under capillary forces.

We used external valves to control the flow on the chip and to generate the droplets on-demand (DOD)³⁴. We opened the core phase supplied under a constant rate of flow q with the continuous phase switched off. After a time Δt we closed the core phase and opened the continuous phase which cut off a droplet of volume $q\Delta t$. Accordingly, by applying a sequence of opening times $\Delta t_1, \Delta t_2, \dots, \Delta t_N$ of the valves we could generate

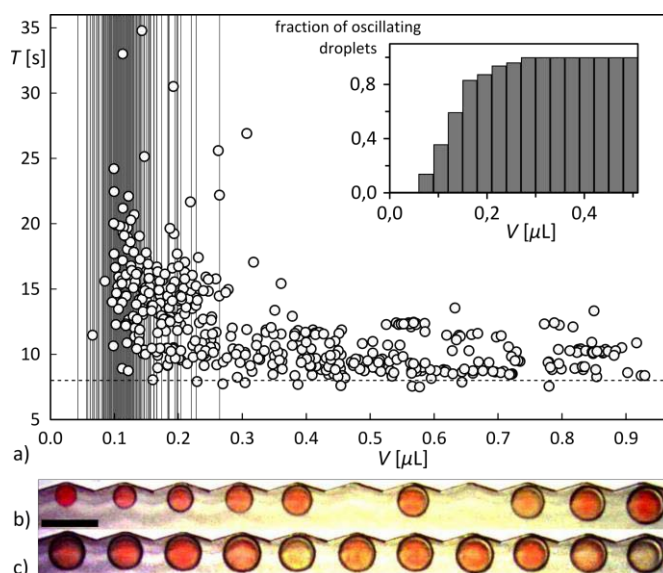


Fig. 2. (a) Period of oscillation T of a BZ-droplet encapsulated inside an oil capsule (5mg/mL solution of asolectin in hexadecane) plotted against the volume of the BZ-droplet. The data were collected from approx. 60 independent experiments (altogether over 600 droplets). The vertical lines correspond to volumes at which the droplets did not oscillate at all. The horizontal dashed line indicates the period 8 s observed for a large ($V > 1 \mu\text{L}$) reference BZ-droplet suspended directly in bulk oil (for details see main text). Inset shows the fraction of oscillating droplets observed within the indicated volume intervals. Snapshots (b-c) show arrays of droplets with the droplets having either gradually increasing volume (b) or constant volume (c). In case (b), previous to locking inside the traps, the droplets travelled along the channel with various speeds resulting in varying spacing between them and thus in some of the traps being empty. In case (c) all traps were filled with droplets. On the snapshot (c) one can also see that the oscillations of various droplets are out of phase. We did not observe any interaction (e.g., synchronization of oscillations) between the capsules. The scale bar is 2 mm.

an arbitrary sequence of volumes of the cores ($q\Delta t_1, q\Delta t_2, \dots, q\Delta t_N$).

In order to generate multiple droplets we used three immiscible liquids: the BZ solution as the encapsulated core phase, 5mg/mL solution of asolectin (Sigma-Aldrich)—a mixture of lipids from soy containing around 76% unsaturated fatty acids—in hexadecane (99%, Sigma Aldrich; density $\rho_{hex} = 0.77 \text{ kg/dm}^3$, kinematic viscosity $\nu_{hex} = 3.9 \text{ cSt}$) as the shell phase, and fluorocarbon oil (3M Novec Engineered Fluid 7500; density $\rho_f = 1.61 \text{ kg/dm}^3$, kinematic viscosity $\nu_f = 0.77 \text{ cSt}$) as the external continuous phase. The chemical composition of the core phase was: 0.3 M H_2SO_4 , 0.125 M $\text{CH}_2(\text{COOH})_2$, 0.04 M KBr, 0.00013 M $\text{Ru}(\text{bpy})_3\text{Cl}_2$, 0.375 M NaBrO_3 and 0.00125 M $[\text{Fe}(\text{batho})_3]^{2+}$. The purpose of using the lipids in the shell phase was twofold. First, lipid monolayers adsorbed at the surface of aqueous droplets stabilizing them against coalescence. Second, the double bonds C=C in the unsaturated hydrocarbon tails of the lipids reacted with the BZ-inhibitor bromine diffusing outside the BZ-droplets. As a result, the inhibitory coupling between droplets was reduced with respect to the activatory coupling caused by the diffusion of the HBrO_2 molecules. This in turn enabled propagation of the chemical wave-fronts

through the membranes.¹⁹ In order to better visualize formation of the membranes we performed an additional control experiment in which we dispersed BZ droplets directly in the lipid solution, and poured the emulsion into a Petri dish where the droplets sedimented and formed a quasi 2D system at the bottom of the dish. The contacts between the drops could readily be seen as bright lines, and one could also distinguish finite contact angles between the droplets (see Fig. S1). In literature, those two features are known to be signatures of a formation of a bilayer^{18, 27, 35}. We observed passing of the chemical waves through these connections and no passing where no connections were formed.

We used fluorocarbon as the external phase because its interfacial tension with oil ($\gamma_{f-o}=1.7\pm 0.1$ mN/m; measured by a pendant drop method) is by almost two orders of magnitude smaller than its interfacial tension with the aqueous BZ-medium, which we roughly assume to be the same as with pure water ($\gamma_{BZ-f}=49.5\pm 0.5$ mN/m)³⁶, which promotes spontaneous wetting of BZ-droplets by oil^{9, 37} and provides stable encapsulation. In addition, fluorocarbon preferentially wets the walls of the channels and can carry both aqueous and oil droplets. If one were interested to work with the multiple droplets in an aqueous continuous liquid, this could be done by using a suitable method of patterning the wettability of the channels³⁸.

We assume that the different shells do not interact chemically. Indeed, as discussed above, the lipids contained in the shell phase effectively bind the BZ-inhibitor. On the other hand the disproportionation of BZ-activator is rapid³⁹ and thus the diffusion of HBrO₂ through the fluorocarbon phase cannot lead to effective propagation of excitations at long distances. However, even in the case if some of the BZ-messengers diffused inside the external phase, the distances ($l \approx 1$ mm) between different shells were large enough to prevent communication at the relevant timescale. Assuming the diffusion constant in fluorocarbon²¹ $D_f = 10^{-5}$ cm²/s the characteristic time of communication between the shells equals $t = l^2/D_f \sim 10^3$ s, which is by around two orders of magnitude larger than the typical period of oscillations of the BZ-cores in our experiment (see Fig. 2). Thus, we conclude that the networks of droplets encapsulated in different shells can be treated as independent.

The use of automated generation of double droplets⁹ to produce compartments containing BZ reagents posed several challenges. First, it is known that the BZ reaction generates a gaseous product. Expanding bubbles introduce unwanted residual flow that spoils the control over the automated formulation of droplets in the microfluidic junctions. Following the work by Thutupalli et al.¹⁸ we decided to split the BZ solution into two stocks: A (H₂SO₄, CH₂(COOH)₂, KBr and ruthenium complex) and B (NaBrO₃ and [Fe(batho)₃]²⁺) which mixed directly on chip (see Fig. 1).

In addition we decided to deposit the components A and B inside two independent chambers on the chip. Each stream underwent a 1:2 (v/v) dilution inside the chip when a BZ droplet was formed. We induced the flow of both components

by pushing the liquids with an externally supplied immiscible liquid phase (for this purpose we used fluorocarbon oil FC40).⁴⁰ This allowed us to change the composition of the BZ solution by refilling the chambers directly by hand from a syringe, without the need for cleaning the whole external setup i.e., the external pressurized chambers, valves and long (~2m) steel capillaries that stabilize the flow rates.⁴¹ The period of BZ oscillations is a complex function of concentration of reagents.⁴² Our setup allowed for easy modification of the concentrations of the substrates and thus the frequency of chemical oscillations in droplets within a single experiment.

In order to prevent wetting of the walls of the microchannels by the aqueous and oil phases we applied a commercial perfluorinated coating (3M Novec 1720) which rendered the polycarbonate walls both hydrophobic and oleophobic. We kept the inlet chambers for A and B components of the BZ medium non-modified in order to prevent wetting in this region by the 'pushing' fluorinated FC40 phase. Otherwise we observed capillary rise of FC40 along the corners of the chamber towards the T-junction, an effect that compromised our ability to control the process of formation of droplets. We used FC40 rather than Novec 7500 for pushing the BZ phase because it was less likely to completely wet the walls of the channels.

Some of our experiments required generation of large BZ droplets, i.e., such that their length in the narrow channel upstream the chamber exceeded 20 times the width of the channel. In such a case we observed fragmentation of the droplets at the usual step-like inlet to the chamber by the so-called step emulsification mechanism.⁴³ We prevented this unwanted fragmentation by redesigning the inlet to the chamber to have a smooth profile with an opening angle α of around 30 degrees (see Fig. 1). In order to prevent merging of the cores in case of doublet structures, we used the ruthenium complex (Ru(bpy)₃Cl₂) as an additional catalyst that increased mechanical stability of droplets inside the capsule.

Our experiments required immobilization of capsules in their metastable morphologies for at least 15 minutes. For this purpose we exploited buoyancy of the drops (the external fluorocarbon phase was approximately twice denser than the capsules) and engraved notches at the side wall of the observation chamber. These notches served as geometric traps (Fig. 1). After tilting the device to the side of the chamber, buoyancy locked the capsules in the notches. The tilt angle of the order of few degrees was sufficient to immobilize the capsules without disturbing their shape. By using a microscope with a field of view of 3 cm in diameter we could observe up to 15 capsules at the same time.

Results.

Shells with one core (singlets).

For the concentrations considered, we checked that the period of the BZ oscillation in a bulk solution not covered by oil equals 11 s. In the case of large droplets (i.e., with diameter

<http://rcin.org.uk>

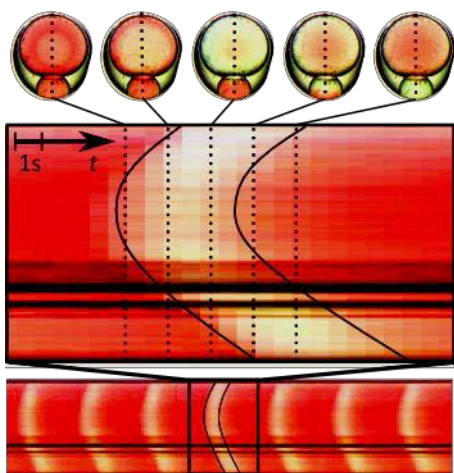


Fig. 3. Cuts of the snapshots of a BZ-doublet along the dotted lines (top) collected on a single time-plot (middle and bottom). One can notice parabolic shape of the white stripe representing the chemical wave of the oxidized catalyst expanding from the center of the larger droplet (the black solid lines are guide to the eye) because in the center concentration of activator first exceeds the threshold for self-excitation. The wave propagates outwards, passes through the facet between the droplets and propagates through the small drop. The long-time dynamics can be inferred from a stack containing multiple sequences of oscillations (bottom).

$D > 1$ mm) prepared by simple mixing of the BZ solution with the lipid solution we observed the period of appr. 8 s. Next, we generated arrays of core-shell structures on-chip and incubated them for an interval long enough to determine the period of the chemical oscillations of the active core (Fig. 2a). We repeated the experiment for various volumes of the encapsulated BZ droplets, with their volume ranging between $V = 0.04$ μL (diameter ≈ 0.4 mm; the uncertainty of the diameter stems due from deformation of the droplet from perfectly spherical shape to its buoyancy; in the calculation of diameter we neglect this deformation) and $V = 0.93$ μL ($D \approx 1.2$

mm).

Independently of the volume of the core we kept the volume fraction ϕ of the aqueous phase in the capsule constant ($\phi \approx 0.6$). For droplets, with $V \geq 0.4$ μL ($D \geq 0.9$ mm) we observed an increasing fraction of longer periods and for $V \leq 0.3$ μL increasing fraction of droplets non-oscillating at all.

Finally,

at $V < 0.07$ μL ($D \leq 0.5$ mm) no oscillations were detected. We

believe that different phenomena can be responsible for this effect. Steinbock and Muller⁴⁴ explained the effect by reactions between organic radicals and oxygen diffusing from the oil phase. Our experiments were performed for different concentrations of BZ reagents and another type of oil. We attribute the increase in oscillation period to faster diffusion of

activator (HBrO_2) from a BZ droplet through the lipid membrane to the oil phase inside the shell. The diffusion reduces concentration of the activator inside the aqueous droplet, thus for small droplets, due to larger surface-to-volume ratio, a longer time is needed to attain concentration required for self-excitation. For very small droplets, diffusion is efficient enough to keep activator concentration below the critical value,

so the droplets do not show any oscillations at all. Similar trends have been previously observed for freely suspended droplets⁴⁵ as well as for reactors embedded in gelatin⁴⁶.

The above explanation was also confirmed in an experiment in which we first observed the small droplets not to oscillate for ca. 4 minutes. We subsequently merged the shells by directly contacting them (via tilting the chip towards the inlet to the chamber) such that a single capsule formed with $N=9$ BZ-cores. After merging the shells the cores started to oscillate and those in the interior of the structure developed significantly larger frequency than the peripheral ones. We concluded that the limiting size for oscillations depends also on the number and relative configuration of the encapsulated, neighbouring cores. We note remarkable statistical variations of the period of oscillation (CV of around 15% at the plateau, i.e., for $V \geq 0.4$ μL , see Fig. 2a). We can attribute these deviations

to

the complexity of the BZ-reaction and associated sensitivity of the period to variations in the concentration of the reagents (due to mixing on-chip), possible changes of temperature (e.g., due to heating from the light source) or interaction of BZ-medium with polycarbonate and/or with the hydrophobic coating. We usually observed much smaller variations in the period (CV less than 5% at the plateau) within a single run of the experiment which typically involved observation of around 10 droplets for 15 mins (see Fig. S1 in SI). Thus we expect that providing more robust long-lasting conditions on-chip, achievable by e.g., monitoring the temperature and improving the reproducibility of mixing conditions could yield more precise measurements.

Shells with two cores (doublets).

In the second series of experiments we encapsulated *two* BZ droplets of different sizes in a single shell (Fig. 3). We generated arrays of identical doublets and repeated the experiments for various ratios of sizes of the encapsulated cores. For each doublet we observed formation of a stable facet between the droplets immediately after relaxation of the structure to its metastable shape. Within approximately one minute of formation of the double droplet, chemical communication between initially independently oscillating droplets was typically established manifest by synchronization of the oscillations. As we observed for the case of singlets (Fig. 2a), the frequency of oscillations should increase with increasing volume of the droplet. Thus, we can expect that in a communicating pair of droplets of different volumes the high frequency oscillations in the large droplet should produce spikes of activator that diffuse through the lipid bilayer to the smaller droplet and force excitations inside it (Fig. 3). The time evolution of periodically forced medium can be very complex.⁴⁷⁻⁴⁹ In order to track the propagation of the chemical wave-front between the cores we measured the intensity of the pixels along the line connecting their centers. We recorded such lines of pixels frame by frame obtaining a graphical time-cut through the video. On the graph, the oscillations of the droplets can be seen as nearly white strokes. The lines which bend with their ends pointing in the direction of the arrow of time (as in the large droplet in Fig. 3) correspond to waves of the oxidized

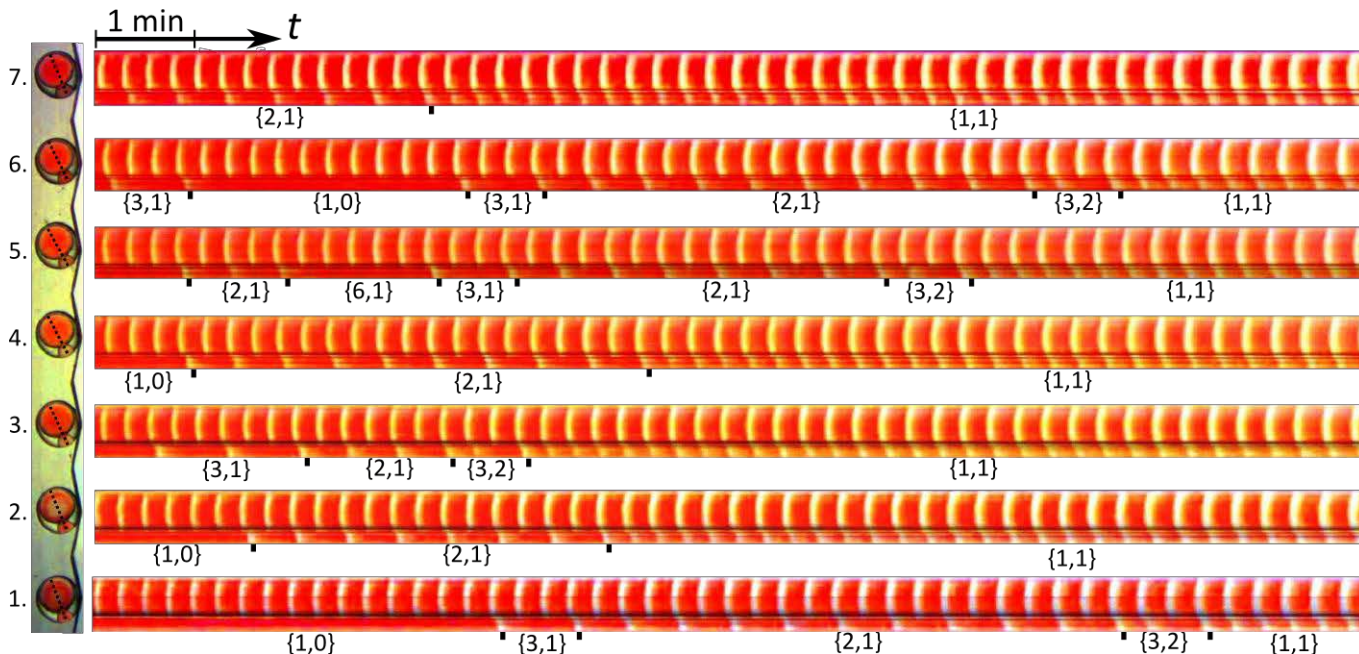


Fig. 4 Time evolution of dynamic patterns in BZ doublets composed of a large ($V=0.9$) and a small droplet ($V=0.08$). The time intervals according to the order of generation) were generated in appr. 10 s intervals. The video recording starts approximately 1 min after generation of the last droplet (no. 7).

catalyst propagating from the middle of the droplet outwards, i.e. these lines correspond to the ‘self-induced’ oscillations. The tilted, non-bent lines correspond to ‘neighbour-induced’ signals passing through a droplet (see the smaller droplet in Fig. 3). The firing number n_L of a small droplet and n_S being the total number of stimuli coming from the large droplet (spikes of the activator), depends on the excitation frequency and on the quality of chemical connection between the compartments. We typically observed that the larger droplet oscillated with its self-induced frequency $f_L = f_{self}$ (as if it had no neighbour) and the smaller droplet oscillated with a frequency f_S that was forced by the large one such that eventually $f_S = f_L$, i.e. the smaller droplet oscillated faster than in the singlet configuration, i.e., $f_S > f_{self}$. Interestingly, even in

the case

of both droplets being large (but not equal), i.e., with almost the same self-frequencies ($V \geq 0.4$), see Fig. 2a), we

still

observed propagation of the signal from the larger to the smaller drop. The only exception was the case of almost identical droplets, i.e., differing in volume by less than 5%. In such cases we observed that either one of the droplets in the pair (we call them X and Y, where Y is generated first) initiated the wave (those were either ‘X’ or ‘Y’ modes, see Fig. S2 in SI), or otherwise that the droplets oscillated strictly in-phase (‘XY’ mode). Interestingly, we also observed transitions between the different modes with time that were probably related to different consumption of reagents. The final quasi-stationary states (i.e., stationary within the time of observation) were 4 X, 6 Y and 2 XY states (we show examples for each case in Fig. S2), from which we can judge that there was a strong preference for the asymmetric state with the ‘inductor’

and a ‘receiver’. The fact that in-phase and neighbour-induced oscillations are dominant for a strong coupling between similar chemical oscillators have been also noticed in the recent studies on synchronicity of BZ gel segments.⁴⁶

In another series of experiments we generated pairs of BZ-droplets with one of the cores significantly smaller than the other. In all experiments the volume of large droplet was around $0.9 V_L$. Intriguing dynamic patterns developed when

the volume V of the smaller core fell near to the regime of vanishing self-induced oscillations ($V \lesssim 0.1 V_L$, as shown in the inset in Fig. 2a). We observed that for such small droplets, not every excitation of the larger droplet activated the smaller one. Instead, we observed commensurate frequencies obeying the relation $f_S/f_L = n_S/n_L = n_S/n_L$. We observed various

patterns $\{n_L, n_S\}$ and transitions between them. In Fig. 4 we analyze an experiment in which we simultaneously tracked the dynamics of 7 independent doublets. Same as in Fig. 3, we used a time-plot of the intensity of the pixels.

Fig. 4 shows the general trend that the smaller droplets pick-up the frequency of the larger ones over time, i.e.,

increases over time. The differences between individual cases can be related to small differences in volumes of encapsulated droplets, but in our opinion they also reflect stochasticity in formation of the membranes through which communication occurs. We typically observed the transition $\{2,1\} \rightarrow \{1,1\}$, i.e. from a situation in which the smaller droplet oscillated with a half of frequency of the larger droplet to oscillations with the

same frequency. The differences between individual cases can be related to small differences in volumes of encapsulated droplets, but in our opinion they also reflect stochasticity in formation of the membranes through which communication occurs. We typically observed the transition $\{2,1\} \rightarrow \{1,1\}$, i.e. from a situation in which the smaller droplet oscillated with a half of frequency of the larger droplet to oscillations with the

same period. In some cases these two patterns were separated by an intermediate one {3,2}. We also observed rather unstable {3,1} patterns (typically lasting one or two periods) as well as periods when there were no oscillations in the small droplet,

<http://rcin.org.pl>

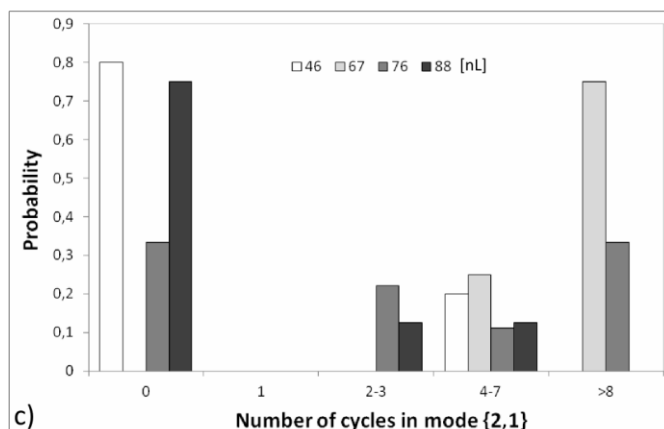
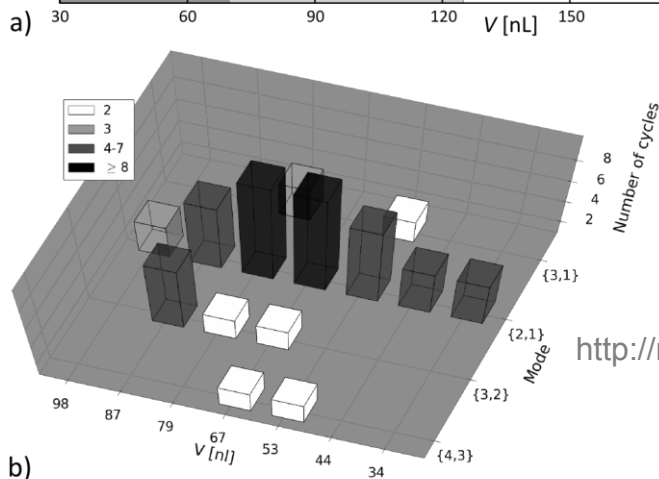
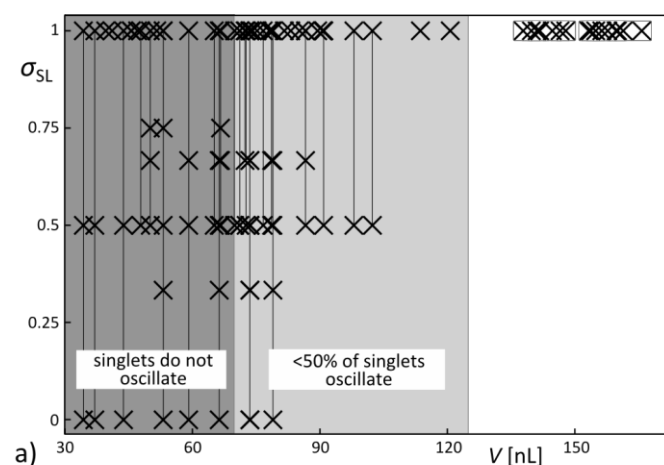


Fig. 5. a) A plot showing the firing number σ_{SL} measured in doublets containing a large and a small droplet, for various volumes V of the

smaller droplet. The vertical lines connect points corresponding to the same droplet. The shaded regions indicate, for comparison, regimes of limited self-induced oscillations (<50% of cases; $V < 125$ nL) and with no oscillations ($V < 70$ nL) in the case of singlets (see inset in Fig. 2a). b) The number of cycles for various dynamic patterns observed in a few selected capsules with different volumes of the small droplet. c) The probability distribution of a number of cycles of oscillation within the {2,1} mode plotted for four different volumes of the small droplet. The average time in which a doublet is in the {2,1} mode was equal to 15,4 s, 225,3 s, 114,4 s and 26 s for volumes of the smaller droplet: 46 nL, 67 nL, 76 nL and 88 nL, respectively.

which we denote by {1,0}. In some cases we observed more complex dynamics. For example the droplet no. 5 in Fig. 4

developed quite complex pattern $\{2,1\} \rightarrow \{6,1\} \rightarrow \{3,1\} \rightarrow \{2,1\} \rightarrow \{3,2\} \rightarrow \{1,1\}$. For all droplets the stable final pattern was {1,1} so each oscillation of the large droplet forced excitation of the small one.

It is known that generally the firing number increases when the frequency of arriving excitations decreases.⁴⁷ Here, we can relate the observed increase of the firing number in time to the increase of oscillation period in a large droplet caused by depletion of reagents. For example in the capsule 1 on Fig. 4 the initial period is 14 s, next it increases to 16 s in {2,1} pattern and for {1,1} pattern it is already 18 s. In Fig. 5a we collected all the values σ_{SL} observed over time for various

volumes V of the smaller drop. The vertical lines on the plot connect points corresponding to various patterns for the same droplet (typically the larger values correspond to later time). Only for the volumes smaller than approx. 100 nL we observed patterns different than {1,1}, whereas in this range of volumes for the singlets we rarely observed oscillations of droplets at all (compare with Fig. 2a).

The information of Fig. 5a is extended in Fig. 5b that plots the number of cycles for which a given mode is observed. We collected information on the evolution of the frequency of oscillations in a few selected capsules with different volumes of the small droplet. We see that the most complex time dependent communication involving transition between multiple patterns occurs within a narrow range of volumes of the small droplet (between 50 nL and 90 nL).

The microfluidic system that we describe here provides statistical information on the stability of a given pattern. For example, Fig. 5c illustrates the stochasticity in stability of {2,1} pattern as a function of the droplet volume. The probability density that {2,1} pattern appears for a given number of cycles is presented for a few volumes of the small droplet. Both for small volumes ($V = 46 \pm 3$ nL) and for large ones ($V = 88 \pm 3$ nL) the {2,1} pattern is only occasionally observed, as it does not appear in more than 70% of cases. For the intermediate volumes 67 ± 3 nL and 76 ± 3 nL the probability that this mode appears (i.e., the sum of probabilities for positive numbers of cycles plotted in Fig. 5c) is in both cases higher than 0.65. The average interval of time within which the doublet remains in the {2,1} communication pattern has a pronounced maximum around $V = 70$ nL.

Discussion and conclusions

We demonstrated an automated droplet microfluidic system for studies of chemical communication between liquid compartments of different volumes. We encapsulated droplets containing a reaction-diffusion medium inside an oil shell which served as a mobile 'trap' for the reactive cores. We subsequently immobilized multiple shells by using a specific geometry of the microfluidic channel which allowed for long-time (tens of minutes) observation of oscillation patterns developing between the cores. To our best knowledge, we provide the first experimental report on how resonances

between chemical oscillators depend on the relative volumes of the oscillators.

Shells containing a single BZ-core, at the volumes of the core larger than 0.4 μL showed a roughly constant period

of

oscillations similar to the value of 8 s for large droplets (over 1 μL) suspended in bulk oil. Small droplets of volumes below

0.4

μL exhibited increasingly larger periods for smaller volumes.

Below volumes of roughly 70 nL oscillations vanished.

Already the simplest network comprising two droplets produced various resonance frequencies. Their occurrence was strongly coupled to the relative size of the droplets. Automation of precise generation of capsules containing reacting cores allowed us to investigate the stability of various dynamic patterns against variations in droplet volumes.

Studying the complex dynamics of such 'frequency transformers', besides being interesting from the point of view of basic non-equilibrium statistical mechanics, could be potentially useful in designing future bio-compatible 'smart' microdevices. It has already been shown that structures composed of interconnected droplets communicating via membrane proteins can perform simple functions being analogues of a diode, light sensor, battery or a wave rectifier.⁴

⁵⁰ Our study shows that using a reaction-diffusion medium can add new functionalities. For example, the fact that the excitation of a larger droplet always induces the excitation of the smaller one could be used to direct chemical signals in long ducts (analogues of neurons) composed possibly of hundreds of droplets. We recently reported assembly of linear droplet networks in which the signal is transmitted in a predesigned direction.⁵¹

The present work demonstrates that the systems for on-demand generation of multiple droplets can provide a tool for studies of complex dynamic chemical systems including systems for chemical information processing. Naturally, the information processing functionality increases with the number of interacting cores. It has been shown recently^{15, 52} that clusters built from a few independent compartments of a reaction-diffusion medium can be used as AND, OR, NAND, or XOR logic gates. Such digital logics offers a playground for research on chemical information processing and on perspectives for construction of computers operating in aqueous environment. Assembling such logic gates typically requires precise positioning of several modules into a predesigned 2D topology. We recently shown how DOD technique in combination with capillary self-assembly can be used to construct given 2D topologies, also those involving droplets of various volumes.⁹ In the present work we show that those tools can also be used in the case of droplets containing reactive BZ-mixture. As such, simple droplet-based logic gates seem to be within reach of current droplet-microfluidics techniques.

Finally, we note that the system that we presented is suitable to studying the properties of lipid bilayers composed of various kinds of lipids. For example by using reservoirs with

two kinds of lipids and changing composition from capsule to capsule our technique could be used to screen hundreds of various compositions in a single run of the experiment.⁴⁰ We

<http://rcin.org.pl>

expect that the type of lipid can influence the oscillations at least two-folds: i) via changing the rate of diffusion of the activator outside the droplet and ii) via changing the lag time (time of diffusion through the membrane); the latter could be sensitive not only to a type of lipid but also fluidity of the membrane (depending on temperature, tension, etc.). We leave this rich and interesting subject for future investigation. Such kind of studies could be particularly useful in assessing optimal conditions for trans-membrane transport as well as the probability of membrane protein insertion, which are both of fundamental interest in general biology and physiology.

Acknowledgements

Project financed by the European Research Council Starting Grant 279647 and via the European Regional Development Fund under the Operational Programme Innovative Economy NanoFun POIG.02.02.00-00-025/09. J.G. acknowledges financial support from Ministry of Science under the grant Iuventus Plus IP2012 012472 and Mobility Plus 1058/MOB/2013/0.

Notes and references

^a *Institute of Physical Chemistry, Polish Academy of Sciences, ul. Kasprzaka 44/52, 03-982 Warsaw, Poland.* <http://rcin.org.pl>

^b *current address: Department of Mechanical and Aerospace Engineering, Princeton University, Princeton, New Jersey 08544, USA.*

* email: garst@ichf.edu.pl

† Electronic Supplementary Information (ESI) available. See DOI: 10.1039/b000000x/

1. M. H. J. Saier and T.-T. Tseng, in *Transport of molecules across microbial membranes*, ed. S. B. J.K. Broome-Smith, C.J. Stirling and F.B. Ward, Cambridge University Press, Cambridge, UK, 1999, pp. 252-274.
2. G. J. Kaczorowski, O. B. McManus, B. T. Priest and M. L. Garcia, *Journal of General Physiology*, 2008, **131**, 399-405.
3. M. J. Spooner and P. A. Gale, *Chemical Communications*, 2015, **51**, 4883-4886.
4. M. A. Holden, D. Needham and H. Bayley, *Journal of the American Chemical Society*, 2007, **129**, 8650-8655.
5. K. Funakoshi, H. Suzuki and S. Takeuchi, *Analytical Chemistry*, 2006, **78**, 8169-8174.
6. N. Malmstadt, M. A. Nash, R. F. Purnell and J. J. Schmidt, *Nanoletters*, 2006, **6**, 1961-1965.
7. A. S. Utada, E. Lorenceau, D. R. Link, P. D. Kaplan, H. A. Stone and D. A. Weitz, *Science*, 2005, **308**, 537-541.
8. T. Nisisako, S. Okushima and T. Torii, *Soft Matter*, 2005, **1**, 23-27.
9. J. Guzowski, S. Jakiela, P. M. Korczyk and P. Garstecki, *Lab on a Chip*, 2013, **13**, 4308-4311.
10. G. Villar, A. J. Heron and H. Bayley, *Nature Nanotechnology*, 2011, **6**, 803-808.
11. A. Adamatzky, B. De Lacy Costello and T. Asai, *Reaction-Diffusion Computers*, Elsevier, New York, 2005.
12. K. Yoshikawa, I. N. Motoike, T. Ichino, T. Yamaguchi, Y. Igarashi, J. Gorecki and J. N. Gorecka, *International Journal of Unconventional Computing*, 2009, **5**, 3-37.
13. J. Gorecki and J. N. Gorecka, in *Encyclopedia of Complexity and Systems Science*, ed. R. A. Meyers, Springer, Berlin, 2009.
14. R. J. Field and R. M. Noyes, *Journal of Chemical Physics*, 1974, **60**, 1877-1884.

15. J. Holley, I. Jahan, B. De Lacy Costello, L. Bull and A. Adamatzky, *Physical Review E*, 2011, **84**, 056110.
16. <http://neu-n.eu>.
17. J. Szymanski, J. N. Gorecka, Y. Igarashi, K. Gizynski, J. Gorecki, K.-P. Zauner and M. de Planque, *International Journal of Unconventional Computing*, 2011, **7**, 185-200.
18. S. Thutupalli, S. Herminghaus and R. Seeman, *Soft Matter*, 2011, **7**, 1312-1320.
19. S. Thutupalli and S. Herminghaus, *European Physical Journal E*, 2013, **36**, 91.
20. M. Toiya, V. K. Vanag and I. R. Epstein, *Angewandte Chemie-International Edition*, 2008, **47**, 7753-7755.
21. J. Delgado, N. Li, M. Leda, H. O. Gonzalez-Ochoa, S. Fraden and I. R. Epstein, *Soft Matter*, 2011, **7**, 3155-3167.
22. N. Tompkins, N. Li, C. Girabawe, M. Heymann, G. B. Ermentrout, I. R. Epstein and S. Fraden, *Proceedings of the National Academy of Sciences of the United States of America*, 2014, **111**, 4397-4402.
23. S. Jakiela, S. Makulska, P. M. Korczyk and P. Garstecki, *Lab on a Chip*, 2011, **11**, 3603-3608.
24. J. Guzowski, P. M. Korczyk, S. Jakiela and P. Garstecki, *Lab on a Chip*, 2011, **11**, 3593-3595.
25. M. Zagnoni, *Lab on a Chip*, 2012, **12**, 1026-1039.
26. S. Ota, H. Suzuki and S. Takeuchi, *Lab on a Chip*, 2011, **11**, 2485.
27. A. R. Thiam, N. Bremond and J. Bibette, *Langmuir*, 2012, **28**, 6291-6298.
28. M. Zagnoni and J. M. Cooper, *Lab on a Chip*, 2010, **10**, 3069-3073.
29. M. A. Czekalska, T. S. Kaminski, S. Jakiela, K. T. Sapra, H. Bayley and P. Garstecki, *Lab on a Chip*, 2015, **15**, 541-548.
30. K. Churski, P. Korczyk and P. Garstecki, *Lab on a Chip*, 2010, **10**, 816-818.
31. F. Rossi, A. Zenati, S. Ristori, J.-M. Noel, V. Cabuil, F. Kanoufi and A. Abou-Hassan, *International Journal of Unconventional Computing*, 2015, **11**, 23-36.
32. R. Tomasi, J.-M. Noel, A. Zenati, S. Ristori, F. Rossi, V. Cabuil, F. Kanoufi and A. Abou-Hassan, *Chemical Science*, 2014, **5**, 1854-1859.
33. J. Szymanski, J. Gorecki and J. B. Hauser, *Journal of Physical Chemistry C*, 2013, **117**, 13080-13086.
34. K. Churski, J. Michalski and P. Garstecki, *Lab on a Chip*, 2010, **10**, 512-518.
35. C. E. Stanley, K. S. Elvira, X. Z. Niu, A. D. Gee, O. Ces, J. B. Edel and A. J. deMello, *Chemical Communications*, 2010, **46**, 1620-1622.
36. Q. Brosseau, J. Vignon and J.-C. Baret, *Soft Matter*, 2014, **10**, 3066-3076.
37. N.-N. Deng, W. Wang, X.-J. Ju, R. Xie, D. A. Weitz and L.-Y. Chu, *Lab on a Chip*, 2014, **14**, 3428-3429.
38. A. R. Abate, D. Lee, T. Do, C. Holtze and D. A. Weitz, *Lab on a Chip*, 2008, **8**, 516-518.
39. F. Ariese and Z. Ungvarainagy, *Journal of Physical Chemistry*, 1986, **90**, 1-4.
40. K. Churski, T. S. Kaminski, S. Jakiela, W. Kamysz, W. Baranska-Rybak, D. B. Weibel and P. Garstecki, *Lab on a Chip*, 2012, **12**, 1629-1637.
41. S. Jakiela, P. M. Korczyk, S. Makulska, O. Cybulski and P. Garstecki, *Physical Review Letters*, 2012, **108**, 134501.
42. J. Gorecki, J. Szymanski and J. N. Gorecka, *Journal of Physical Chemistry A*, **115**, 8855-8859.
43. R. Dangla, S. C. Kayi and C. N. Baroud, *Proceedings of the National Academy of Sciences of the United States of America*, 2013, **110**, 853-858.
44. O. Steinbock and S. C. Muller, *Journal of Physical Chemistry A*, 1998, **102**, 6485-6490.
45. J. Szymanski, J. N. Gorecka, Y. Igarashi, K. Gizynski, J. Gorecki, K.-P. Zauner and M. De Planque, *International Journal of Unconventional Computing*, 2011, **7**, 185-200.
46. P. R. Buskohl, R. C. Kramb and R. A. Vaia, *Journal of Physical Chemistry B*, 2015, **119**, 3595-3602.
47. J. Siewewiesiuk and J. Gorecki, *Journal of Physical Chemistry A*, 2002, **106**, 4068-4076.
48. J. Siewewiesiuk and J. Gorecki, *Physical Chemistry Chemical Physics*, 2002, **4**, 1326-1333.
49. J. Siewewiesiuk and J. Gorecki, *Physical Review E*, 2002, **66**, 016212.
50. G. Maglia, A. J. Heron, W. L. Hwang, M. A. Holden, E. Mikhailova, Q. Li, S. Cheley and H. Bayley, *Nature Nanotechnology*, 2009, **4**, 437-440.
51. J. Gorecki, K. Gizynski, J. Guzowski, J. N. Gorecka, P. Garstecki, G. Gruenert and P. Dittrich, *Philosophical Transactions of the Royal Society a-Mathematical Physical and Engineering Sciences*, 2015, **373**, 20140219.
52. J. Gorecki, J. N. Gorecka and A. Adamatzky, *Physical Review E*, 2014, **89**, 042910.